Chemical Science

ROYAL SOCIETY OF CHEMISTRY

EDGE ARTICLE

View Article Online
View Journal | View Issue

Cite this: *Chem. Sci.*, 2022, **13**, 8412

All publication charges for this article have been paid for by the Royal Society of Chemistry

Received 21st March 2022
Accepted 29th June 2022

DOI: 10.1039/d2sc01622b

rsc.li/chemical-science

Highly efficient organic long persistent luminescence based on host–guest doping systems†

Yunhan Zhao, Bingbing Ding, * Zizhao Huang and Xiang Ma *

Recently, organic long persistent luminescence (OLPL) has attracted widespread attention as a new luminescence pathway initiated by the exciplex. However, the low quantum yield, few alternative molecules and high fabrication cost seriously slow down the development of OLPL materials. Herein, a series of simple multi-guest/host OLPL materials with a high quantum yield are reported by doping four phenothiazine derivative guest molecules into 9*H*-xanthen-9-one host matrices. The F-substituted phenothiazine derivative doping system displays highly efficient emission with 46.3% quantum yield in air. Meanwhile, these OLPL materials provide broad opportunities for further application in the field of heat resistance due to their highly efficient luminescence at high temperatures.

Introduction

In recent years, organic photoluminescent materials showing long-lived emission have aroused great interest of researchers. There are three categories of organic materials that can exhibit long-lived emission. One is thermally activated delayed fluorescence (TADF),[1] one is room-temperature phosphorescence (RTP), and the other is organic long persistent luminescence (OLPL). TADF has a relatively short lifetime, mostly in the microsecond range. Pure organic room-temperature phosphorescence (RTP) materials show great potential in optical sensing,[2,3] light-emitting diodes,[4,5] imaging probes,[6–9] and information encryption and storage[10–13] due to their long emitting lifetime (microseconds to even seconds) with large Stokes shifts and low manufacturing cost. Considerable efforts are devoted to the enhancement of the RTP performance of crystalline packaged systems[14–20] and amorphous pure organic RTP systems.[21–26] However, its serious drawback is that it is easily quenched by oxygen[27] and difficult to obtain at high temperatures.

In 2017, Adachi and co-workers[28] reported the first OLPL system of two simple organic molecules, free from metal elements, and can generate OLPL that lasts for more than one hour at room temperature. The most significant difference between RTP and OLPL is that RTP is realized by singlet exciton spin-flipping to the triplet state through intersystem crossing and the triplet excitons return to the singlet state in the form of radiative transitions, while OLPL is realized by the intermediate charged state. RTP and OLPL can be distinguished by the form of lifetime decay.[29] The emission decay mode of RTP systems always exhibits exponential decay since there is no energy storage mechanism. In contrast, power-law decay is exhibited by the emission decay mode of OLPL systems due to the existence of an intermediate charged state. The formation of the exciplex is the key factor for OLPL. The performance of OLPL has been thoroughly studied in the next few years. In 2018, the characteristics of OLPL were improved by doping emitter molecules into an OLPL matrix.[30] Multi-color emissions were achieved by energy transfer from the exciplex in the OLPL matrix to the emitter dopants. Furthermore, a polymer-based OLPL system that was flexible, transparent, and solution processable was developed.[31] In 2021, research[32] showed that amorphous OLPL systems could be excited by radiation up to 600 nm and exhibited a yellow-to-NIR LPL emission in air. However, present room-temperature OLPL materials usually need an expensive molecule such as 2,8-bis(diphenylphosphoryl)dibenzo[*b*,*d*]thiophene (PPT) as the acceptor. Except for lifetime, quantum yield is another essential performance parameter of an OLPL system for its various potential applications to ensure that the OLPL signal can be detected not only by instrument but also by the naked eye. Although some progress has been made in the field of OLPL[33–37] in recent years, low quantum yield and high preparation cost are still hurdles in most reported OLPL systems, and developing facilely prepared OLPL materials with a high quantum yield has been still an urgent challenge to be overcome.

In this work, four highly efficient yellow-green OLPL systems (Φ_{PL} 23.1%, 46.3%, 23.0%, and 23.1%) (Fig. S25–S28†) were

Key Laboratory for Advanced Materials, Feringa Nobel Prize Scientist Joint Research Center, Frontiers Science Center for Materiobiology and Dynamic Chemistry, Institute of Fine Chemicals, School of Chemistry and Molecular Engineering, East China University of Science and Technology, Meilong Road 130, Shanghai 200237, P. R. China. E-mail: maxiang@ecust.edu.cn; bbding@ecust.edu.cn

† Electronic supplementary information (ESI) available. See https://doi.org/10.1039/d2sc01622b

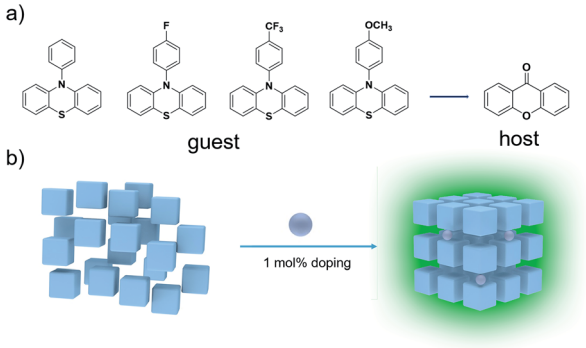

Fig. 1 (a) Molecular structure of different guests and host matrices. (b) Schematic illustration of the host/guest doping strategy.

obtained by doping four simple molecules (Fig. 1, namely H-PzPh, F-PzPh, CF_3-PzPh, and OCH_3-PzPh) with weak blue emission as guests into host (9*H*-xanthen-9-one) molecules that show extremely weak luminescence with a 1% molar ratio. The synthetic route and characterization are shown in Fig. S1–S16.† The specific method is to completely dissolve the host and guest in dichloromethane to obtain a transparent mixed solution, and then evaporate the organic solvent under vacuum and fully dry. To the best of our knowledge, 46.3% of the F-PzPh doping system is a fairly high quantum yield for reported OLPL systems. In addition to the form of lifetime decay, another feature that is significantly different from phosphorescence is that this OLPL material possesses excellent high temperature resistance and still maintains highly efficient emission even at 90 °C, which is conducive to the construction of heat-resistant materials.

Results and discussion

According to UV-vis absorption spectra, four guest molecules and their doping systems showed wide absorption peaks at 250–370 nm (Fig. S17†). As shown in Fig. 2a and b, the H-PzPh guest molecule mainly exhibited fluorescence emission at 445 nm without phosphorescence, and when doped into the host matrices at a 1% molar ratio, a new 535 nm delayed emission peak appeared. This new delayed emission peak didn't originate from the host because the host emission peak was located at 450 nm (Fig. S20†). The other guest molecules (F-PzPh, CF_3-PzPh, and OCH_3-PzPh) exhibited 445 nm fluorescence emission and weak phosphorescence emission (520 nm, 520 nm, and 510 nm, respectively). When doped into the host matrices at a 1% molar ratio, there was only one emission peak (530 nm, 520 nm, and 540 nm, respectively). The quantum yield of all crystalline (Fig. S23†) doping systems was greatly improved compared to individual guests (Table 1). Moreover, the F-doping system was selected to explore the influence of different doping molar ratios on the luminescence intensity and emission decay of OLPL materials due to the highest quantum yield. As shown in Fig. 2c and d, with the increase of the doping ratio (from 0.1% to 5%), the emission intensity showed the trend of first rising and then falling. The 1 mol% doping ratio offered the system the strongest emission intensity and the longest duration time.

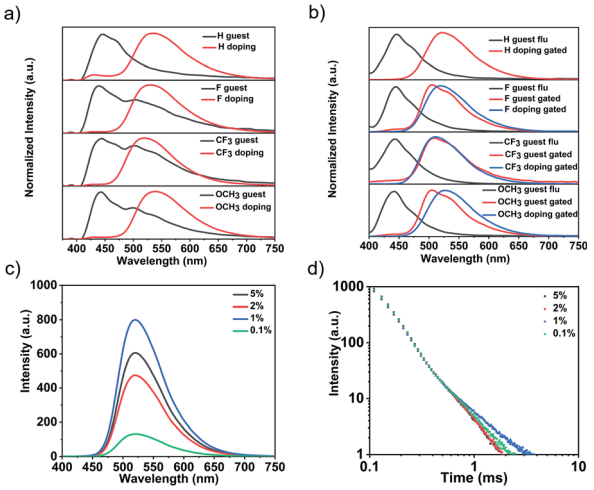

Fig. 2 (a) Normalized photoluminescence spectra of H-PzPh, F-PzPh, CF_3-PzPh, and OCH_3-PzPh powder and corresponding doping powder. Excitation wavelength: 330 nm. (b) Normalized fluorescence and gated-emission spectra (delay time = 0.1 ms) of H-PzPh, F-PzPh, CF_3-PzPh, and OCH_3-PzPh powder and corresponding doping powder. Excitation wavelength: 330 nm. (c) Gated-emission spectra (excitation slim = emission slim = 10 nm; excitation voltage = 700 V; delay time = 0.1 ms) of the F-doping system with different molar ratios. Excitation wavelength: 330 nm. (d) Emission decay profiles of the F-doping system with different molar ratios monitored at 530 nm.

To prove that the delayed emission of the doping system was not thermally activated delayed fluorescence, the emission decay profiles of the four doping systems were tested from room temperature to 77 K (Fig. S21†). The results showed that the lifetime of each doping system increased with the decrease of temperature, so the possibility of TADF was excluded. The delayed spectrum and lifetime (Fig. S22†) of the guest molecules in toluene solution at 77 K also indirectly ruled out the possibility of TADF. As shown in Fig. 3, except for the H-PzPh guest molecule (no RTP), the emission decay profiles of the other guest molecules exhibited exponential decay attributed to RTP properties. As a comparison, the emission decay profiles of all doping systems exhibited power-law decay[38–40] attributed to OLPL properties. Unlike most long duration time OLPL systems, the duration time of our system is relatively short. Therefore, the emission decay profiles of different delay times

Table 1 Optical properties of H-PzPh, F-PzPh, CF_3-PzPh, and OCH_3-PzPh powder and corresponding doping powder (1 mol%)[a]

	λ_F nm^{-1}	λ_p nm^{-1}	λ_{LPL} nm^{-1}	Φ_{PL}
H-PzPh	445	N.D.	N.D.	2.9%
H-PzPh doping	N.D.	N.D.	535	23.1%
F-PzPh	445	520	N.D.	2.3%
F-PzPh doping	N.D.	N.D.	530	46.3%
CF_3-PzPh	445	520	N.D.	3.3%
CF_3-PzPh doping	N.D.	N.D.	520	23.1%
OCH_3-PzPh	445	510	N.D.	3.7%
OCH_3-PzPh doping	N.D.	N.D.	540	23.0%

[a] N.D.: not detected.

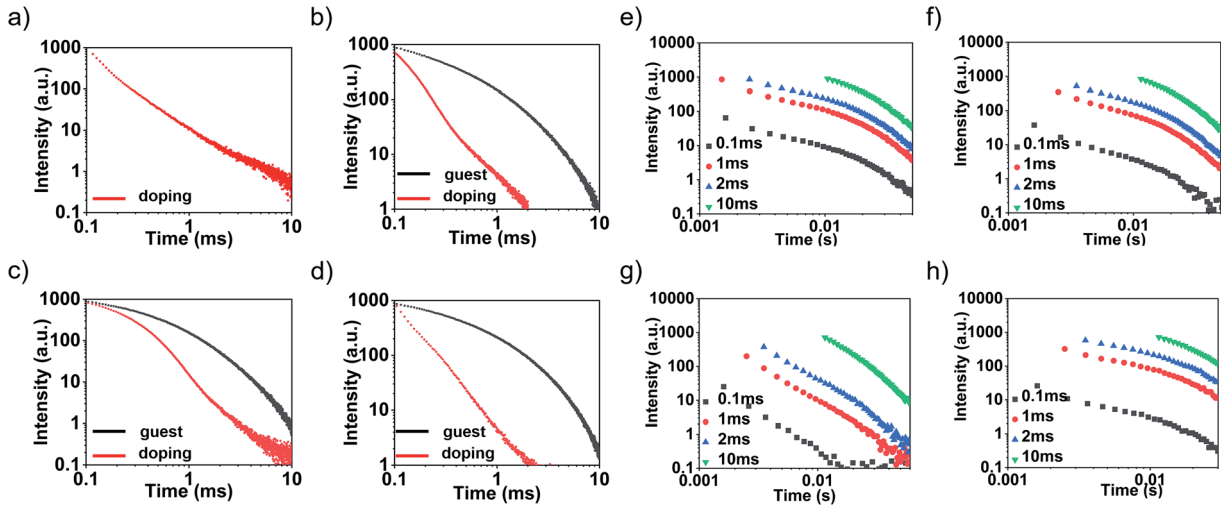

Fig. 3 (a–d) Emission decay profiles of different guests and corresponding doping systems (delay time = 0.1 ms). (e–h) Emission decay profiles of different doping systems with different delay times. (a and e) H-PzPh monitored at 535 nm, (b and f) F-PzPh monitored at 530 nm, (c and g) CF_3-PzPh monitored at 520 nm and (d and h) OCH_3-PzPh monitored at 540 nm.

(0.1 ms, 1 ms, 2 ms, and 10 ms, respectively) were tested to further prove that this type of luminescence was attributed to OLPL. Experimental results showed that the emission decay (even delay time = 10 ms) was still in accord with the power-law decay rule, which proved that these doping systems were still OLPL systems. In other words, there was a phenomenon of rapid emission attenuation for these doping systems, which made it difficult to capture the luminous intensity by the naked eye in the later stage of the attenuation.

We calculated the highest occupied molecular orbital (HOMO) level and the lowest unoccupied molecular orbital (LUMO) level distributions of the four guest and host molecules (Fig. 4a). The energy level matching of the HOMO and LUMO is the prerequisite for OLPL. The matching principle is that the HOMO of the guest is higher than the HOMO of the host but lower than the LUMO of the host, and the LUMO of the guest is higher than the LUMO of the host.[28] As shown in Fig. 4b, due to the HOMO and LUMO energy level match between guest molecules and host molecules, after photo-excitation, electrons are transferred from the HOMO of the guest molecules to the HOMO of the host molecules to form charge-transfer states. Then, charge-separated states are formed due to host free radical anion diffusion resulting in guest free radical cations moving away from host free radical anions. Furthermore, radical cations and radical anions recombine gradually. Charge recombination of the host radical anions and the guest radical cations generates exciplexes in a ratio of 25% singlet exciplexes and 75% triplet exciplexes (Fig. 4c). Finally, the exciplex emission is generated in the transitions from the LUMO of host molecules to the HOMO of guest molecules.

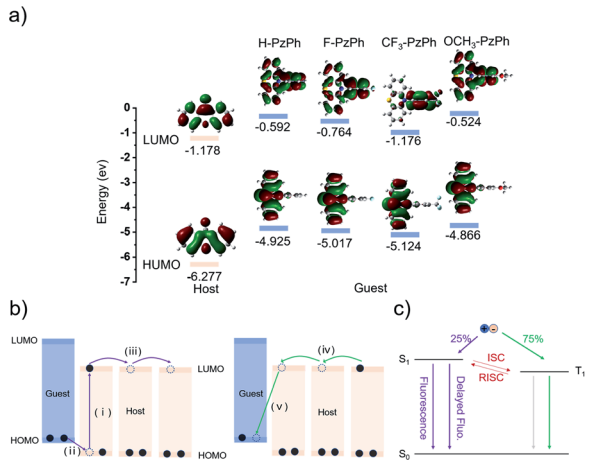

Fig. 4 (a) The frontier molecular orbit of H-PzPh, F-PzPh, CF_3-PzPh and OCH_3-PzPh and host molecules. (b) Emission mechanism of OLPL systems. Five processes: (i) photoexcitation, (ii) charge transfer, (iii) charge separation, (iv) charge recombination and (v) exciplex emission. (c) The path of exciplex emission. ISC: inter-system crossing; RISC: reverse inter-system crossing.

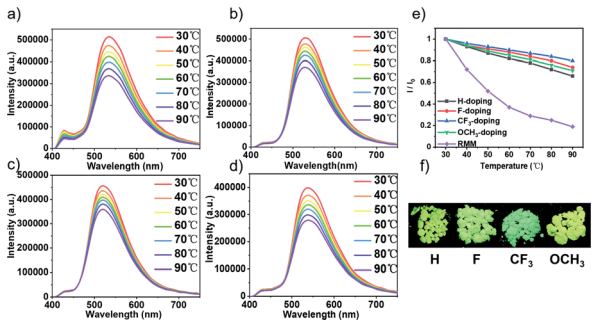

Fig. 5 Photoluminescence spectra at different temperatures of the (a) H-doping system, (b) F-doping system, (c) CF_3-doping system and (d) OCH_3-doping system. Excitation wavelength: 330 nm. (e) The quenching ratio of the four OLPL systems and RMM phosphorescence system at different temperatures (H-doping monitored at 535 nm, F-doping monitored at 530 nm, CF_3-doping monitored at 520 nm, OCH_3-doping monitored at 540 nm, and RMM monitored at 570 nm). (f) Luminescence images of the four doping systems illuminated with 365 nm UV lamps at 90 °C.

To develop organic heat-resistant long-lived luminescence materials, the influence of temperature was also explored on doping systems' performance. Fig. 5a–d show that remarkable high temperature resistance was exhibited by all doping materials. As shown in Fig. 5e, the CF_3-doping system showed the best luminescence resistance to high temperature, and the emission intensity at 90 °C was only reduced by 20.3% compared with that at 30 °C. The emission intensity of other doping systems was not decreased by much either (H-doping system 33.8%, F-doping system 26.2%, and OCH_3-doping system 29.5%, respectively). As a contrast, the phosphorescence intensity of the phosphorescence material RMM[41] (constructed from β-CD and malic acid in a molar ratio of 1 : 15 with the doping Bromonaphthimide dye) was 80% lower at 90 °C than at 30 °C. Heat-resistant luminescence is a major advantage of our OLPL materials compared to phosphorescence materials. As shown in Fig. 5f, all doping systems could still maintain excellent comprehensive performance at 90 °C (great thermal stability and highly efficient luminescence), which provides an important reference for the construction of heat-resistant materials.

Conclusions

In summary, a series of high quantum yield OLPL materials were obtained by doping four guest molecules (H-PzPh, F-PzPh, CF_3-PzPh, and OCH_3-PzPh) into a host molecule (9*H*-xanthen-9-one) at a molar ratio of 1%. In particular, the F-doping system showed a fairly high Φ_{PL} of 46.3%. It was proved by emission decay profiles and a low temperature experiment that this type of luminescence belonged to OLPL induced by an exciplex instead of TADF and RTP. Furthermore, the importance of energy level (HOMO and LUMO) matching between guest molecules and host molecules for OLPL was illustrated by frontier orbital theory. In addition, these OLPL materials maintained strong emission intensity and thermal stability even at high temperature (90 °C), which offers a new idea for designing heat-resistant luminescence materials that are clearly visible to the naked eye.

Author contributions

Y. Zhao and X. Ma proposed the project and designed the lab experiments. Y. Zhao implemented the preparation of materials and photophysical experiments and analyzed the experimental results. Y. Zhao and X. Ma cowrote the manuscript. B. Ding help to revise the manuscript. Z. Huang offered advice on drawing pictures.

Conflicts of interest

There are no conflicts to declare.

Acknowledgements

The authors gratefully acknowledge the financial support from the National Natural Science Foundation of China (21788102, 22125803, 22020102006, and 21871083), a project support by the Shanghai Municipal Science and Technology Major Project (Grant No. 2018SHZDZX03), the Program of Shanghai Academic/Technology Research Leader (20XD1421300), the "Shu Guang" project supported by the Shanghai Municipal Education Commission and Shanghai Education Development Foundation (19SG26), and the Fundamental Research Funds for the Central Universities.

Notes and references

1 H. Uoyama, K. Goushi, K. Shizu, H. Nomura and C. Adachi, *Nature*, 2012, **492**, 234–238.
2 X. Yao, J. Wang, D. Jiao, Z. Huang, O. Mhirsi, F. Lossada, L. Chen, B. Haehnle, A. J. C. Kuehne, X. Ma, H. Tian and A. Walther, *Adv. Mater.*, 2021, **33**, 2005973.
3 W. Li, Q. Huang, Z. Mao, J. Zhao, H. Wu, J. Chen, Z. Yang, Y. Li, Z. Yang, Y. Zhang, M. P. Aldred and Z. Chi, *Angew. Chem., Int. Ed.*, 2020, **59**, 3739–3745.
4 W. Ratzke, L. Schmitt, H. Matsuoka, C. Bannwarth, M. Retegan, S. Bange, P. Klemm, F. Neese, S. Grimme, O. Schiemann, J. M. Lupton and S. Hoger, *J. Phys. Chem. Lett.*, 2016, **7**, 4802–4808.
5 T. Wang, X. Su, X. Zhang, X. Nie, L. Huang, X. Zhang, X. Sun, Y. Luo and G. Zhang, *Adv. Mater.*, 2019, **31**, 1904273.
6 J. Wang, Z. Huang, X. Ma and H. Tian, *Angew. Chem., Int. Ed.*, 2020, **59**, 9928–9933.
7 Q. Dang, Y. Jiang, J. Wang, J. Wang, Q. Zhang, M. Zhang, S. Luo, Y. Xie, K. Pu, Q. Li and Z. Li, *Adv. Mater.*, 2020, **32**, 2006752.
8 V. N. Nguyen, Y. Yim, S. Kim, B. Ryu, K. M. K. Swamy, G. Kim, N. Kwon, C. Y. Kim, S. Park and J. Yoon, *Angew. Chem., Int. Ed.*, 2020, **59**, 8957–8962.
9 H. J. Yu, Q. Zhou, X. Dai, F. F. Shen, Y. M. Zhang, X. Xu and Y. Liu, *J. Am. Chem. Soc.*, 2021, **143**, 13887–13894.
10 Y. Su, S. Z. F. Phua, Y. Li, X. Zhou, D. Jana, G. Liu, W. Q. Lim, W. K. Ong, C. Yang and Y. Zhao, *Sci. Adv.*, 2018, **4**, eaas9732.
11 J. X. Wang, Y. G. Fang, C. X. Li, L. Y. Niu, W. H. Fang, G. Cui and Q. Z. Yang, *Angew. Chem., Int. Ed.*, 2020, **59**, 10032–10036.
12 Z. Y. Zhang and Y. Liu, *Chem. Sci.*, 2019, **10**, 7773–7778.
13 X. K. Ma and Y. Liu, *Acc. Chem. Res.*, 2021, **54**, 3403–3414.
14 Z. Yang, Z. Mao, X. Zhang, D. Ou, Y. Mu, Y. Zhang, C. Zhao, S. Liu, Z. Chi, J. Xu, Y. C. Wu, P. Y. Lu, A. Lien and M. R. Bryce, *Angew. Chem., Int. Ed.*, 2016, **55**, 2181–2185.
15 B. Ding, L. Ma, Z. Huang, X. Ma and H. Tian, *Sci. Adv.*, 2021, **7**, eabf9668.
16 T. Nishiuchi, H. Sotome, R. Fukuuchi, K. Kamada, H. Miyasaka and T. Kubo, *Aggregate*, 2021, **2**, e126.
17 S. Garain, S. Kuila, B. C. Garain, M. Kataria, A. Borah, S. K. Pati and S. J. George, *Angew. Chem., Int. Ed.*, 2021, **60**, 12323–12327.
18 L. Gu, H. Shi, L. Bian, M. Gu, K. Ling, X. Wang, H. Ma, S. Cai, W. Ning, L. Fu, H. Wang, S. Wang, Y. Gao, W. Yao, F. Huo, Y. Tao, Z. An, X. Liu and W. Huang, *Nat. Photonics*, 2019, **13**, 406–411.

19 Y. Wang, J. Yang, Y. Tian, M. Fang, Q. Liao, L. Wang, W. Hu, B. Z. Tang and Z. Li, *Chem. Sci.*, 2019, **11**, 833–838.
20 Y. Lei, J. Yang, W. Dai, Y. Lan, J. Yang, X. Zheng, J. Shi, B. Tong, Z. Cai and Y. Dong, *Chem. Sci.*, 2021, **12**, 6518–6525.
21 M. S. Kwon, Y. Yu, C. Coburn, A. W. Phillips, K. Chung, A. Shanker, J. Jung, G. Kim, K. Pipe, S. R. Forrest, J. H. Youk, J. Gierschner and J. Kim, *Nat. Commun.*, 2015, **6**, 8947.
22 D. Li, F. Lu, J. Wang, W. Hu, X. M. Cao, X. Ma and H. Tian, *J. Am. Chem. Soc.*, 2018, **140**, 1916–1923.
23 Z. Wang, T. Li, B. Ding and X. Ma, *Chin. Chem. Lett.*, 2020, **31**, 2929–2932.
24 Y. Li, F. Gu, B. Ding, L. Zou and X. Ma, *Sci. China: Chem.*, 2021, **64**, 1297–1301.
25 Y. Zhang, Y. Su, H. Wu, Z. Wang, C. Wang, Y. Zheng, X. Zheng, L. Gao, Q. Zhou, Y. Yang, X. Chen, C. Yang and Y. Zhao, *J. Am. Chem. Soc.*, 2021, **143**, 13675–13685.
26 W. Huang, X. Zhang, B. Chen, H. Miao, C. O. Trindle, Y. Wang, Y. Luo and G. Zhang, *Chem. Commun.*, 2018, **55**, 67–70.
27 X. Ma, J. Wang and H. Tian, *Acc. Chem. Res.*, 2019, **52**, 738–748.
28 R. Kabe and C. Adachi, *Nature*, 2017, **550**, 384–387.
29 N. Nishimura, Z. Lin, K. Jinnai, R. Kabe and C. Adachi, *Adv. Funct. Mater.*, 2020, **30**, 2000795.
30 K. Jinnai, R. Kabe and C. Adachi, *Adv. Mater.*, 2018, **30**, 1800365.
31 Z. Lin, R. Kabe, N. Nishimura, K. Jinnai and C. Adachi, *Adv. Mater.*, 2018, **30**, 1803713.
32 K. Jinnai, R. Kabe, Z. Lin and C. Adachi, *Nat. Mater.*, 2022, **21**, 338–344.
33 J. Han, W. Feng, D. Y. Muleta, C. N. Bridgmohan, Y. Dang, G. Xie, H. Zhang, X. Zhou, W. Li, L. Wang, D. Liu, Y. Dang, T. Wang and W. Hu, *Adv. Funct. Mater.*, 2019, **29**, 1902503.
34 L. Xiao, Z. Wang, C. Zhang, X. Xie, H. Ma, Q. Peng, Z. An, X. Wang, Z. Shuai and M. Xiao, *J. Phys. Chem. Lett.*, 2020, **11**, 3582–3588.
35 W. Li, Z. Li, C. Si, M. Y. Wong, K. Jinnai, A. K. Gupta, R. Kabe, C. Adachi, W. Huang, E. Zysman-Colman and I. D. W. Samuel, *Adv. Mater.*, 2020, **32**, 2003911.
36 X. Liang, Y. X. Zheng and J. L. Zuo, *Angew. Chem., Int. Ed.*, 2021, **60**, 16984–16988.
37 P. Alam, T. S. Cheung, N. L. C. Leung, J. Zhang, J. Guo, L. Du, R. T. K. Kwok, J. W. Y. Lam, Z. Zeng, D. L. Phillips, H. H. Y. Sung, I. D. Williams and B. Z. Tang, *J. Am. Chem. Soc.*, 2022, **144**, 3050–3062.
38 W. H. Hamill, *J. Chem. Phys.*, 1979, **71**, 140–142.
39 M. Yamamoto, H. Ohkita, W. Sakai and A. Tsuchida, *Synth. Met.*, 1996, **81**, 301–304.
40 H. Ohkita, T. Koizumi, W. Sakai, T. Osako, M. Ohoka and M. Yamamoto, *Chem. Phys. Lett.*, 1997, **276**, 297–302.
41 S. Sun, J. Wang, L. Ma, X. Ma and H. Tian, *Angew. Chem., Int. Ed.*, 2021, **60**, 18557–18560.